Fish and Shellfish Immunology 100 (2020) 334–344

Contents lists available at ScienceDirect

Fish and Shellfish Immunology

journal homepage: www.elsevier.com/locate/fsi

Full length article

Histological mucous cell quantification and mucosal mapping reveal different aspects of mucous cell responses in gills and skin of shorthorn sculpins (*Myoxocephalus scorpius*)

Mai Dang[a,b], Karin Pittman[c], Christian Sonne[d,e], Sophia Hansson[d,f], Lis Bach[d], Jens Søndergaard[d], Megan Stride[a], Barbara Nowak[a,d,*]

[a] Institute for Marine and Antarctic Studies, University of Tasmania, Launceston, Tasmania, 7250, Australia
[b] Department of Bacteriology, Institute of Veterinary Research and Development of Central Vietnam, Km 4, 2/4 Street, Vinh Hoa, Nha Trang, Khanh Hoa, 57000, Viet Nam
[c] Department of Biology, University of Bergen, Thormøhlensgate 53, 5006, Bergen, Norway
[d] Aarhus University, Faculty of Science and Technology, Department of Bioscience, Arctic Research Centre (ARC), Frederiksborgvej 399, PO Box, 358, 4000, Roskilde, Denmark
[e] Henan Province Engineering Research Center for Biomass Value-added Products, School of Forestry, Henan Agricultural University, Zhengzhou, 450002, China
[f] Ecolab, Université de Toulouse, CNRS, Avenue de l'Agrobipole, 31326, Castanet Tolosan, France

ARTICLE INFO

Keywords:
Mucosal mapping
Histopathology
Gills
Skin
Mucous cells

ABSTRACT

In teleosts, the mucosal epithelial barriers represent the first line of defence against environmental challenges such as pathogens and environmental contaminants. Mucous cells (MCs) are specialised cells providing this protection through mucus production. Therefore, a better understanding of various MC quantification methods is critical to interpret MC responses. Here, we compare histological (also called traditional) quantification of MCs with a novel mucosal mapping method to understand the differences between the two methods' assessment of MC responses to parasitic infections and pollution exposure in shorthorn sculpins (*Myoxocephalus scorpius*). Overall, both methods distinguished between the fish from stations with different levels of pollutants and detected the links between MC responses and parasitic infection. Traditional quantification showed relationship between MC size and body size of the fish whereas mucosal mapping detected a link between MC responses and Pb level in liver. While traditional method gave numerical density, mucosal mapping gave volumetric density of the mucous cells in the mucosa. Both methods differentiated MC population in skin from those in the gills, but only mucosal mapping pointed out the consistent differences between filament and lamellar MC populations within the gills. Given the importance of mucosal barriers in fish, a better understanding of various MC quantification methods and the linkages between MC responses, somatic health and environmental stressors is highly valuable.

1. Introduction

Assessment of fish health is often based on fish's morphology (including fish biometrics and histology), haematology or measurement of immune responses [1]. Morphological assessment of fish health which is based on measurements of some biometric features (such as length, weight or condition factors) and internal organs (such as liver somatic index or gonad somatic index) is limited in precision and sensitivity [1,2]. Measurement of blood cells and biochemistry can be fraught with interpretational difficulties due to pre-analytical effects [3]. Examination of immune responses can be based on both specific and non-specific responses [1,4]. The first fish defence barrier against all external challenges such as pathogens or environmental contaminants is the mucosal epithelium, a thin layer covering the whole surface area of fish including skin, gills and gut [5–8].

In teleosts, the gills are one of the most important sites of mucous epithelia which account for more than 50% of the fish's surface area and play multiple functions including respiration, osmoregulation, acid-base regulation, cell signalling and iron transport and excretion of nitrogenous waste [9–11]. The gill epithelium is a thin and delicate layer directly exposed to the surrounding environment [12,13]. The structure and function of gills can be altered in response to irritants such as heavy metal, transition metals, low pH, detergent and polycationic agents which make gills a good candidate organ for environmental monitoring programs [14–18].

* Corresponding author. Institute for Marine and Antarctic Studies, University of Tasmania, Launceston, Tasmania, 7250, Australia.
E-mail address: b.nowak@utas.edu.au (B. Nowak).

https://doi.org/10.1016/j.fsi.2020.03.020
Received 13 January 2020; Received in revised form 10 March 2020; Accepted 11 March 2020
Available online 12 March 2020
1050-4648/

Skin is an important interface separating external and internal environments, and preventing the entry of waterborne toxic chemicals and pathogens into fish [7,19]. In contrast to mammalian skin, fish skin is hydrated, non-keratinized and covered by slimy mucus secreted by this living cell layer. All these features make the skin relatively sensitive to waterborne chemicals, physical and biological stressors. However, skin is not a routine target organ or end point for environmental health research although it is a main determinant of fish health [7,19].

In the gills and skin teleosts, the mucosal epithelial barriers act as a living immune, physical and biochemical interface between fish and the environment [7,8,20]. These mucosal barriers contain mucous cells that produce mucins. Other components of mucus can include a number of bioactive components including antimicrobial, antifungal, anti-viral and anti-parasitic compounds such as lysozymes, immunoglobulins, complement, cytokines, acute-phase proteins, carbonic anhydrase, lectins, crinotoxins, calmodulin, C-reactive protein, antimicrobial peptides and hemolysin [7,21–23]. The skin and gill mucosa are in a continuous contact with the external environment and they are sensitive to changes in water quality which make them helpful in fish health assessments.

Two available methods to analyse the state of these mucosal barriers are: i, counts and measurement of MCs in histological sections (traditional method) and ii, mucosal mapping of size and volumetric density of MCs in a mucosal tissue and the barrier status of the tissue (representing tissue activity level) [24–29]. The traditional method has been used to assess MCs responses to anthropogenic stressors [30–32] while the mucosal mapping is a novel objective and quantitative method used to quantify the robustness of the mucous barrier in aquaculture [24,33,34]. Mucosal mapping is derived from design-based stereology for recreation of 3D structures from 2D sections [35] and has been used in environmental monitoring using shorthorn sculpins at the former mining site in Maarmorilik, Greenland [29].

Here we compare routine/traditional quantification with mucosal mapping to uncover the differences between the two methods in assessment of MC responses to environmental challenges including pollution exposure and parasitic infections. We discuss the potential applications of each of the mucosal index as a fish health indicator. Given the important functions of mucosal barriers in fish, a better understanding of various MC quantification methods and potential linkages between MC responses and environmental challenges is valuable for both fisheries and aquaculture.

2. Material and methods

2.1. Study area

Sampling area of this study was around the former Black Angel mine in Maarmorilik, West Greenland (Fig. 1) which was a well-documented example of how inland mining can pollute the surrounding marine environment [36]. During operation period (1973–1990), the mine discharged about 8 million tons of tailings and a large amount of waste rocks into the nearby Affarlikassaa fjord and subsequently caused pollution in this area [37]. Samples were collected at three stations around the mine in August 2017 (Fig. 1). Station 1 (71°7′3.37″ N; 51°15′6.15″ W) was close to the mine and highly polluted with lead (Pb) and zinc (Zn) in sediments. Station 2 (71°7′13.19″ N; 51°21′29.14″ W) and station 3 (71°5′57.57″ N; 51°34′14.03″ W) were located along a distance gradient (5 and 12 km, respectively) away from station 1 and had a lower level of metals in sediment and water. All the sampling sites are very cold areas with temperature ranging from −30 °C to 10 °C. Water temperature was from −2 °C to 5 °C and often covered with ice [37]. Information on water exchange and current [38], geology [39], sedimentation and dispersion rates [40,41] was documented. Levels of heavy metals in sediment, seawater, fish and levels of parasitic infection in sampled fish of this study were reported and discussed in Ref. [29]. The sampled shorthorn sculpin from this area provided an opportunity to inspect the patterns of MC responses in a challenging environment with metal pollution and parasitic infection [29].

2.2. Sample collection

The samples were reused from a previous study on MC responses to pollutants and parasites [29]. Thirty shorthorn sculpins were collected at the three stations (ten fish per station) using fishing rods as described by Ref. [29]. Briefly, the fish were kept alive in seawater and transported to research stations. Fish were handled, euthanised and processed following the Greenland regulations and the permission granted by the Greenland Government to Lis Bach and Jens Søndergaard (project number 771020). Gill and skin samples for MC quantification were collected immediately post-mortem. The second left gill arch and a piece of skin from the tail of fish were collected using scalpel and forceps. The second gill arch on the left was selected as routine histology [42,43] and the tail area of skin was collected because this area was least touched and handled during sample collection (following Quantidoc protocol). These samples were put into pre-labelled histocassettes and fixed using 10% neutral buffered formalin.

2.3. Sample processing and data collection

2.3.1. Traditional count of mucous cells

2.3.1.1. Gills. Histological quantification of MCs on the gills of shorthorn sculpins was conducted only for well-orientated filaments which had an even length of lamellae on both sides of the filament (Fig. 2A). These measurements generated 5 mucosal indices including number of gill MCs per inter-lamellar unit (ILU, H1), number of filament MC per cm of filament (H2), size of filament MCs (H3), number of lamellar MC per cm of lamellae (H4) and size of lamellar MCs (H5).

The number of gill MCs per ILU (H1) was determined as previously described [28]. Five filaments evenly distributed along the gill arch were selected. One fish in each group did not have 5 well-orientated filaments and those fish were excluded from the MC count. The number of MCs between the mid-point (top) of a lamella to the mid-point of the next lamella (the inter-lamellar unit) were counted as routine histology using a light microscope (Nikon Eclipse Ni–U) [42,44]. Data for the other MC indices (H2 – H5) were collected using standard image analysis. 10 photos (10x objective) were captured from the middle of well oriented filaments (but not at the distal end of well-oriented filaments). Lengths of filaments and lamellae were measured as show in Fig. 2A using Image J after calibration of the scale. The number of MCs on either filaments or lamellae were counted using the microscope (10x objective) at the time when the photos were taken. An image of every counted cell was captured using 40x objective to measure the size (Fig. 2C). Threshold and “wand tool” were used to extract the MC area for measurement. The total number of MCs analysed using this method is given in Table 1.

2.3.1.2. Skin. Quantification of skin MCs was conducted based on the previously described method [27] with minor modifications from. Briefly, skin samples were embedded transversally (Fig. 3A), sectioned at 5 μm then stained with PAS/Alcian Blue (pH 2.5) to visualise MCs. Twenty microscopic images of skin (400x) were captured where the epithelium was intact. The number of MCs was counted, and the length of the epidermis was measured in 5 randomly selected images. Data were presented as number of MCs per cm length of epidermis. The size of MCs was measured from the same set of randomly selected images by applying threshold (0, 110–128) on the whole images and using the wand function to select MC area (Image J). The total number of skin MCs measured is included in Table 1.

2.3.2. Mucosal mapping of skin and gills

Fixed samples from all stations were processed using routine histology with tangential orientation of embedding and sectioning (Fig. 2B and D and Fig. 3B). This provides 1–2 square centimetres of surface area for analysis, rather than the traditional 2 square microns obtained by transverse sections

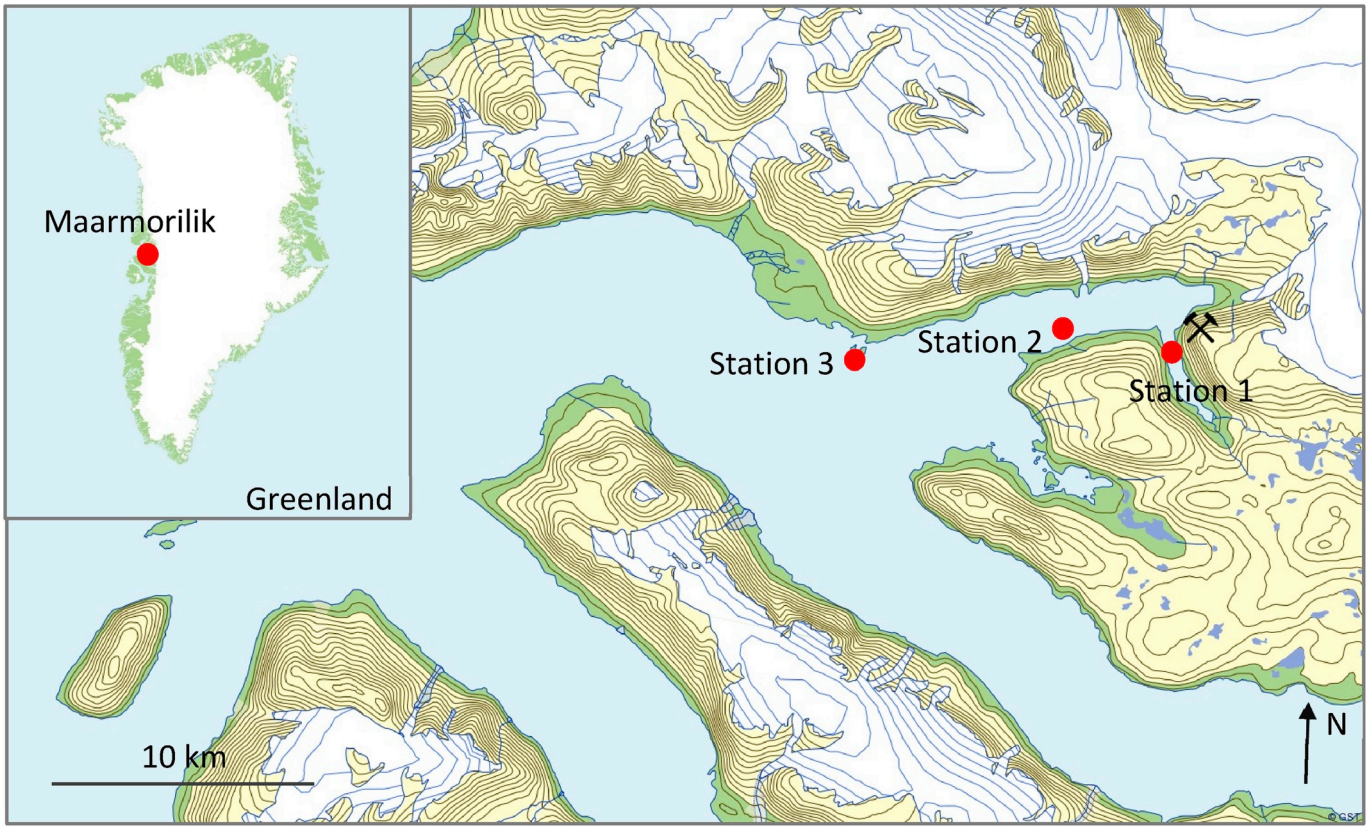

Fig. 1. Sampling stations in Maarmorilik, West-Greenland.

but removes the easy visualization of the component layers. Tangential sections of the gills and skin were stained with Periodic acid Schiff/Alcian Blue (PAS/AB stain, pH 2.5) [24]. The mucosal mapping of sculpin skin and gills was previously described [29] and based on [24,25]. The whole histological sections were scanned using a Leica Axioskop micros microscope connected with the Visiopharm Integrator System (VIS) and a Prior Proscan digital stage. Fifty counter frames (40x) were randomly selected for measurement of MC responses in each organ (skin, gill filaments and gill lamellae) of each fish. Briefly, MC responses were assessed using 3 objective mucosal indices including:

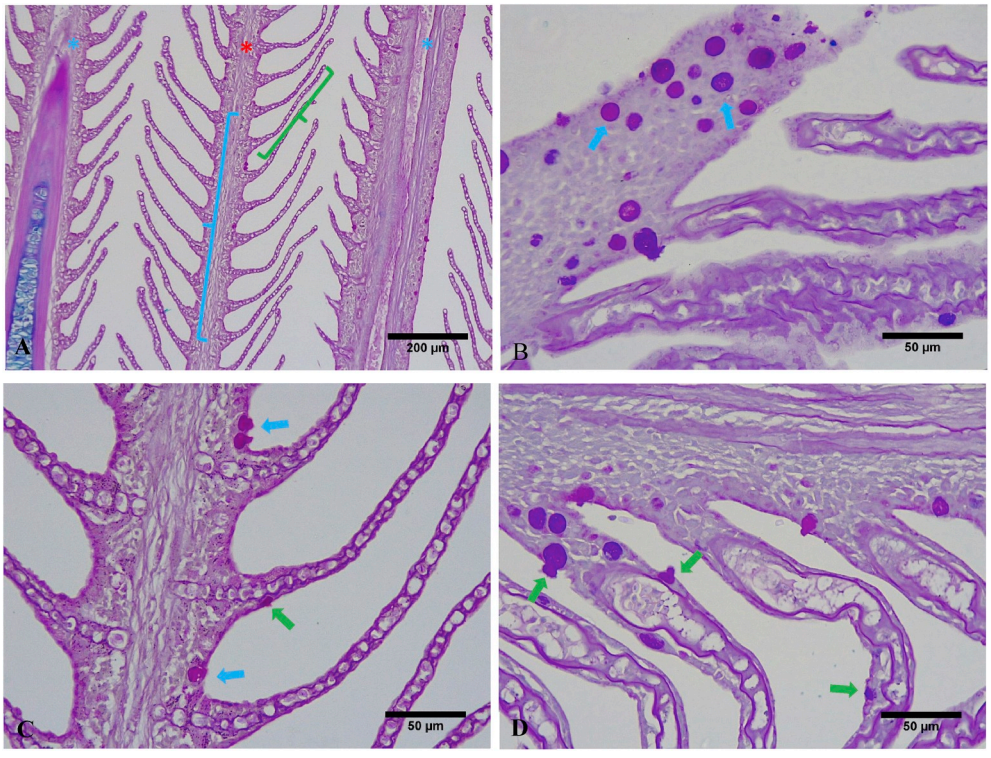

Fig. 2. Quantification of gill mucous cells using traditional method (left images: A and C) and mucosal mapping (right images: B and D) in sculpins from Maarmorilik, West-Greenland. A. Lengths of filament (blue bracket) and lamellae (green bracket) were measured from well-oriented filament (red asterisk). B. Filament mucous cells (blue arrows) were randomly selected from non-well-oriented filament for measurement in mucosal map technique. C. Filament (blue arrows) and lamellae mucous cells (green arrow) in well-oriented filament for measurement in traditional measurement. D. Lamellae mucous cells (green arrows) were randomly selected from non-well-oriented filament for measurement in mucosal map technique. (For interpretation of the references to colour in this figure legend, the reader is referred to the Web version of this article.)

Table 1
Comparison of results from mucosal mapping by Ref. [29]] and traditional measurement in the present study conducted on shorthorn sculpins (n = 26) caught near Maarmorilik (West-Greenland). Yes: statistically significant (P < 0.05). No: not statistically significant (P > 0.05). In mucosal mapping, density is volumetric density (amount of mucosal epithelium filled with mucous cells). ILU = Interlamellar unit, MC = mucous cell.

Method	Mucosal indices	Orientation	Analysed MCs (number)	Measurements per fish (number)	Average values (mean ± SE)			Distinguish between stations	Correlation		
					Station 1	Station 2	Station 3		Body size	Hepatic Pb	Parasites
Traditional method	No MC/ILU (**H1**)	well-oriented	198	10	0.23 ± 0.06	0.08 ± 0.02	0.14 ± 0.04	Yes	Yes	No	No
	No MC/cm filament (**H2**)	well-oriented	336	10	26.67 ± 7.02	22.31 ± 5.74	22.78 ± 6.69	No	Yes	No	No
	Size filament MC (**H3**)	well-oriented	336	13	54.20 ± 3.16	52.84 ± 3.93	40.62 ± 5.63	No	No	No	Yes
	No MC/cm lamellae (**H4**)	well-oriented	59	10	1.96 ± 0.88	0.27 ± 0.19	1.06 ± 0.28	No	Yes	No	No
	Size lamellae MC (**H5**)	well-oriented	59	2	46.68 ± 5.60	41.3 ± 5.62	45.34 ± 7.22	No	Yes	No	No
	No MC/cm skin (**H6**)	transverse	1224	5	310.9 ± 41.5	274.22 ± 30.1	271.11 ± 48.43	No	No	No	No
	Size skin MC (**H7**)	transverse	1224	47	187.16 ± 45.24	227.03 ± 29.18	132.28 ± 15.52	No	Yes	No	No
Mucosal mapping [29]	Filament MC size (**M1**)	not oriented	1948	75	95.53 ± 8.51	84.19 ± 7.59	80.61 ± 6.10	No	Yes	Yes	No
	Filament MC density (**M2**)	not oriented	1948	50	3.62 ± 0.39	2.14 ± 0.47	2.79 ± 0.69	No	No	No	No
	Filament barrier (**M3**)	not oriented	1948	50	0.39 ± 0.04	0.24 ± 0.04	0.32 ± 0.06	No	Yes	No	No
	Lamellar MC size (**M4**)	not oriented	172	7	36.13 ± 8.46	28.52 ± 4.47	36.43 ± 6.40	No	No	Yes	No
	Lamellar MC density (**M5**)	not oriented	172	50	0.24 ± 0.09	0.15 ± 0.02	0.07 ± 0.02	Yes	No	No	No
	Lamellar barrier (**M6**)	not oriented	172	50	0.05 ± 0.02	0.07 ± 0.02	0.03 ± 0.01	No	No	No	No
	Skin MC size (**M7**)	tangential	5788	222	151.04 ± 26.88	203.46 ± 28.14	120.26 ± 11.56	Yes	Yes	No	No
	Skin MC density (**M8**)	tangential	5788	50	3.97 ± 0.99	4.94 ± 0.87	3.72 ± 0.64	No	Yes	No	No
	Skin barrier (**M9**)	tangential	5788	50	0.25 ± 0.03	0.24 ± 0.04	0.13 ± 0.0	No	No	No	Yes

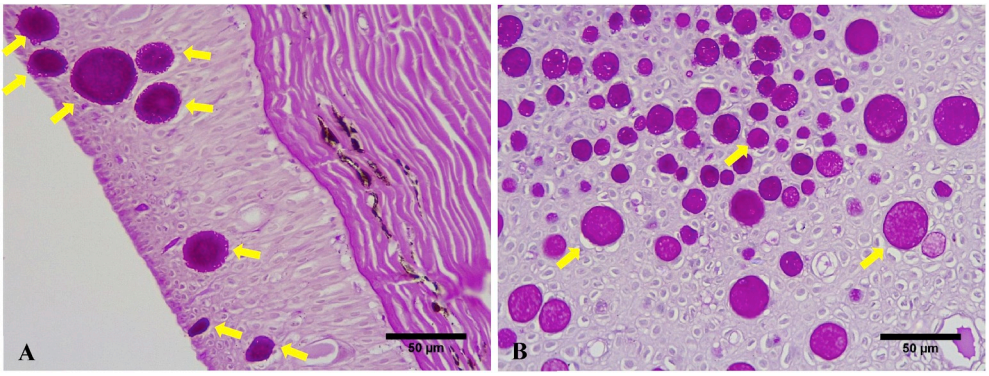

Fig. 3. Quantification of skin mucous cells (pink to purple round cells) using traditional histology (A) methods and mucosal mapping (B) in sculpins from Maarmorilik, West-Greenland. A. Mucous cells (yellow arrows) used for quantification in traditional method. B. Image of epithelium with mucous cells (yellow arrows) achieved from a tangential section of skin used for the mucosal mapping method. (For interpretation of the references to colour in this figure legend, the reader is referred to the Web version of this article.)

(a) Mean MC area was average size of MCs at the equator

(b) Mean MC volumetric density or % mucosal epithelium filled with MCs $= \frac{Mucous\ area\ x\ mucous\ number}{Epithelial\ area} x\ 100$

(c) Barrier status $= \frac{1}{Mucous\ cell\ area\ /\ Mucous\ cell\ density}\ x\ 1000$

The sensitivity of the area measurement is 7 square microns [25], the density goes from 0 to 100% and the Barrier Status ranges in general from 0.01 to about 2.7 for any species or tissue so far (Quantidoc database). From the gills and skin samples, mucosal mapping generated 9 mucosal indices including filament MC size (M1), filament MC volumetric density (M2), filament barrier status (M3), lamellar MC size (M4), lamellar MC volumetric density (M5), lamellar barrier status (M6), skin MC size (M7), skin MC volumetric density (M8) and skin barrier status (M9). The total number of selected and measured MCs by mucosal mapping is shown in Table 1.

2.4. Data analyses

Mucosal mapping quantification data were normally distributed and suitable for standard statistical analyses. Differences between males and females were investigated using an independent Student's t-test (unbalanced samples size, IBM SPSS statistic 22).

For both methods, the effect of exposure to pollutants on MC responses of fish from station 1, 2 and 3 was determined using a one-way ANOVA (IBM SPSS statistic 22). Assumptions of normal distribution and equal variances were checked using histogram and Levene test, respectively. When the assumption was violated, data were log-transformed. Pearson correlation analysis was used to assess potential associations between traditional MC count and mucosal mapping indices, parasitic infections and hepatic Pb levels. $P < 0.05$ was interpreted as statistical significance. Statistical power analyses were performed for all used mucosal indices using G*Power (3.1.9.6). The minimum effect size for all oneway ANOVA test presenting in Table 1 was 0.51 and for Correlation test was 0.495 for Table 1, 0.405 for all test presenting in Table 2 and 0.394 for all test presenting in Table 3. These size effects were considered to be large using Cohen's criteria (1988). With an alpha = 0.05 and power value = 0.8, the sample size used in this study was adequate.

3. Results

The average values (mean ± SE) of each mucosal index based on the traditional methods (H1 – H7) and mucosal mapping (M1 - M9) are presented in Table 1. Results of correlation investigation between these mucosal indices with body size, hepatic Pb and parasitic infections are also summarized in Table 1.

Table 2
Correlation between mucosal indices and body size (n = 26). * indicate significant correlation with $P < 0.05$. ** indicate significant correlation with $P < 0.001$. These correlations were investigated using pooled data even if there were significant differences between stations [29]]. In Mucosal mapping, density is volumetric density (amount of mucosal epithelium filled with mucous cells). ILU = Interlamellar unit, MC = mucous cell.

Method	Mucosal indices		Length	Weight	Liver weight
Traditional method	No MC/ILU (**H1**)	R	0.504**	0.581**	0.657**
		P	0.009	0.002	0.000
	No MC/cm	R	0.424*	0.243	0.323
	filament (**H2**)	P	0.031	0.231	0.107
	Size filament MC	R	0.277	0.374	0.311
	(**H3**)	P	0.171	0.060	0.123
	No MC/cm	R	0.385	0.506**	0.605**
	lamellae (**H4**)	P	0.052	0.008	0.001
	Size lamellae MC	R	0.406*	0.308	0.416*
	(**H5**)	P	0.040	0.126	0.035
	No MC/cm skin	R	0.161	0.132	0.191
	(**H6**)	P	0.433	0.521	0.350
	Size skin MC (**H7**)	R	−0.432*	−0.443*	−0.552**
		P	0.028	0.023	0.003
Mucosal mapping	Filament MC size	R	0.197	0.131	0.190
	(**M1**)	P	0.334	0.523	0.352
	Filament MC	R	0.468*	0.403*	0.421*
	density (**M2**)	P	0.016	0.041	0.032
	Filament barrier	R	0.459*	0.427*	0.425*
	(**M3**)	P	0.018	0.030	0.031
	Lamellar MC size	R	−0.024	−0.013	0.188
	(**M4**)	P	0.908	0.948	0.357
	Lamellar MC	R	0.046	0.149	0.211
	density (**M5**)	P	0.823	0.467	0.300
	Lamellar barrier	R	−0.178	−0.106	−0.170
	(**M6**)	P	0.384	0.605	0.407
	Skin MC size (**M7**)	R	−0.409*	−0.380	−0.460*
		P	0.038	0.056	0.018
	Skin MC density	R	−0.288	−0.317	−0.405*
	(**M8**)	P	0.154	0.115	0.040
	Skin barrier (**M9**)	R	0.147	0.189	0.130
		P	0.472	0.356	0.528

3.1. Traditional count of mucous cells

3.1.1. Station differences

There was no significant difference between stations in the number and size of MCs per cm length filament (H2 and H3), lamellae (H4 and H5) or skin (H6 and H7) (Table 1). However, the fish from station 1 had the highest number of gill MCs/ILU (H1) (0.23 ± 0.06) that was significantly different from station 2 (0.08 ± 0.02) but not from station 3 (0.14 ± 0.04) (Fig. 4, Table 1).

3.1.2. Body size

Several moderate correlations were detected between mucosal

Table 3
Correlation between the two quantification methods (n = 26). * indicate significant correlation with P < 0.05. ** indicate significant correlation with P < 0.001. In Mucosal mapping, density is volumetric density (amount of mucosal epithelium filled with mucous cells). R: correlation coefficient. ILU = Interlamellar unit. MC = mucous cell.

		Filament MC size (M1)	Filament MC density (M2)	Filament barrier (M3)	Lamellar MC size (M4)	Lamellar MC density (M5)	Lamellar barrier (M6)	Skin MC size (M7)	Skin MC density (M8)	Skin barrier (M9)
No MC/ILU (H1)	R	0.269	0.415*	0.394*	0.240	0.235	−0.167	−0.388	−0.360	0.221
	P	0.183	0.035	0.046	0.238	0.247	0.414	0.050	0.071	0.279
No MC/cm filament (**H2**)	R	0.076	0.250	0.277	0.022	−0.046	−0.244	−0.296	−0.216	0.083
	P	0.712	0.217	0.170	0.915	0.824	0.230	0.142	0.289	0.686
Size filament MC (**H3**)	R	0.265	0.274	0.222	0.142	0.356	0.089	0.184	−0.053	0.378
	P	0.191	0.175	0.277	0.490	0.074	0.664	0.368	0.797	0.057
No MC/cm lamellae (**H4**)	R	0.141	0.446*	0.478*	0.130	0.246	0.072	−0.342	−0.263	0.170
	P	0.493	0.023	0.013	0.525	0.225	0.726	0.087	0.194	0.406
Size lamellae MC (**H5**)	R	0.284	0.359	0.294	0.385	0.215	−0.142	−0.274	−0.229	0.129
	P	0.159	0.071	0.145	0.052	0.291	0.489	0.175	0.260	0.530
No MC/cm skin (**H6**)	R	0.129	0.063	0.015	−0.295	0.137	0.186	−0.093	0.221	0.196
	P	0.529	0.760	0.941	0.144	0.505	0.363	0.650	0.278	0.338
Size skin MC (**H7**)	R	−0.093	−0.121	−0.115	−0.197	0.346	0.424*	0.742**	0.626**	0.359
	P	0.651	0.556	0.576	0.335	0.083	0.031	0.000	0.001	0.072

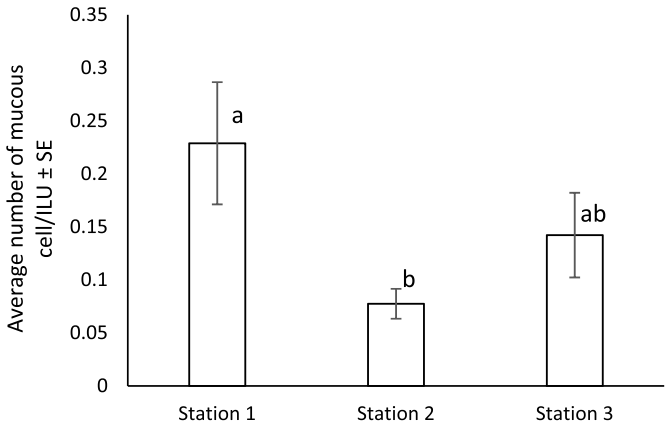

Fig. 4. Average number of mucous cells per interlamellar unit (H1) of the gills of shorthorn sculpin (*Myoxocephalus scorpius*) among three stations near Maarmorilik, West-Greenland. Means with different letters were significantly different from each other.

indices from routine histology and body size (length, weight and liver weight). The number of MCs per ILU (H1), per cm of filament (H2) and per cm of lamellae (H4) positively correlated with body length, weight and/or liver weight (Table 2). The size of lamellar MCs, H5, (but not on filament, H3) was positively correlated with body length and liver weight. By contrast, size of skin MCs (H7) was negatively correlated with all body size indices (Table 2).

3.1.3. Hepatic Pb

No significant correlations were detected between traditional mucosal indices (H1 – H7) and the concentration of Pb in liver of shorthorn sculpins (P > 0.05, Table 1).

3.1.4. Parasitic infections

The size of MCs on the gill filament (H3) was negatively correlated with number of the gill trichodinids (R = −0.512, n = 26, P = 0.007) and skin digenea (R = −0.666, n = 26, P < 0.001, Table 1).

3.1.5. Organ-specific differences

Using traditional histology we found significant differences between MC populations on gills and skin. The size of skin MCs (H7, 180.43 ± 19.65 μm^2) was significantly larger than those of gills (H3 and H5, 46.80 ± 3.11 μm^2) (F = 44, df = 2, p < 0.001). The number of skin MCs (H6, 285.81 ± 23.28 cells/cm length) was significantly greater than those of gills (H2 and H4, 12.55 ± 2.00 cells/cm length) (F = 135.1, df = 2, p < 0.001). It is important to note that density of skin and gill MCs were not directly comparable as the thickness and the structure of the skin or gill epithelium are vastly different even if the "running epithelial length" is the same. There was no difference in the size or number of MCs in the gill filament (H2 and H3) versus in the lamellae (H4 and H5).

3.2. Mucosal mapping

3.2.1. Body size

Filament MC density (M2) and barrier status (M3) were positively correlated with all body size indices (Table 2). Skin MC mean size (M7) and volumetric density (M8) negatively correlated with liver weight and/or body length (Table 2). No correlation was detected between any lamellar mucosal indices (M4, M5 and M6) and body size categories.

3.2.2. Organ-specific differences

MC sizes, volumetric densities and barrier status were organ specific and significantly different. Skin MC size (M7, 158.25 ± 10.97 μm^2) was significantly largest and approximately 2 times larger than those in filaments (M1, 86.78 ± 5.78 μm^2) and 5 times larger than those in lamellae (M4, 33.49 ± 6.07 μm^2) (F = 45.98, df = 2, P < 0.001). The volumetric density of MCs significantly differed for skin and gills. The sculpin skin had a significantly higher density (M8) of MCs with about 4.21 ± 0.61% of epithelium layer filled with MCs in comparison with 2.85 ± 0.65% in the filaments (M2) and 0.15 ± 0.02% of lamellae (M5) (P < 0.001). The skin mucous barrier status (M9) was similar to that of the filament (M3) but differed from that of the lamellae (M6) (F = 54.50, df = 2, P < 0.001). On average, the barrier status of skin and filament was maintained between 0.27 and 0.32 whereas lamellar barrier status was 0.05.

Mucosal mapping detected two distinct populations of MCs in the gills: the filament MCs (relatively large and dense) and those on the lamellae (small and usually sparse). The filament MCs were significantly larger (M1, t = 8.4, df = 58, p < 0.001) and their distribution was denser (M2, t = 9.3, df = 29.6, p < 0.001) than those of the lamellae (M4 and M5) at all stations, suggesting a separate function and/or origin.

3.3. Associations between mucosal mapping and traditional mucous cell counts

The correlations between mucosal mapping (M1 – M9) and

Table 4
Differences between histological quantification of mucous cells and mucosal mapping.

Comparison	Histological quantification of mucous cells	Mucosal mapping (design-based stereology: 3D from 2D)
Length or area included in the analysis	1–2 mm running length of epithelium	1–2 cm^2 surface area
Unit of measure	relative to existing structures (for example interlammelar units)	universally applicable
Orientation of the section	very important	not important
Standardization	no standardized units	standardized reporting
	not directly comparable across treatment and organs	comparable across treatment and organs
Qualitative or quantitative	qualitative and quantitative	quantitative
Method	Manual	semi-automated
Bias	unbiased only if random selection rules followed (see Methods in and [28])	unbiased

traditional MC counts (H1 – H7) are summarized in Table 3. There were moderate positive correlations between number of gill MCs per ILU (H1) and number of MCs per cm lamellae (H4) with volumetric density of MCs on filament (M2) and the barrier status of filament (M3). The histological measure of size of skin MCs (H7) strongly correlated with mucosal mapping skin MC size (M7) and skin MC volumetric density (M8). The mean skin MC size were 187 μm^2 for station 1, 227 μm^2 for station 2 and 132 μm^2 for station 3, in histology whereas they were 151 μm^2 for station 1, 203 μm^2 for station 2 and 120 μm^2 for station 3 in mucosal mapping. The correlation between size of skin MC (H7) and lamellae barrier status (M6) was moderate and positive (Table 3).

4. Discussion

The positive correlations between the traditional method and mucosal map were expected as the two methods measured the same MC populations. However, due to the differences in the selection of analysed areas and measurement techniques (Table 4), the associations between the two methods were ranging from weak to moderate among gill mucosal indices but were strong among skin mucosal indices. This also resulted in the differences between the two methods with regard to their capability to distinguish fish from various sampling sites and organ-specific MC dynamics, and their associations with body size, hepatic Pb and parasitic infection. Results achieved from each analysis are summarized and compared in Table 1. Results from mucosal mapping measurements regarding differences among stations and correlation with hepatic metals and parasitic infections for the same fish were previously reported [29].

The differences in absolute MC sizes are mainly due to the non-random selection of cells to measure in transverse sections of histology, while mucosal mapping applies stereology to estimate cell size at the equator of cells with unbiased selection from tangential sections [45]. This is best shown for the gill filament, where histology measured average cell size as being about half of that obtained by mucosal mapping which estimates cell size at its equator. This outcome is generated from an understanding of the geometry of a sphere: there is one chance to “hit” the equator but 99 chances to hit something between that and the poles (“0” in size). If the equator is equal to 100, then a biased size estimator will generate a mean size of 50 as the mean between 100 and 0 [46]. In the case of both the skin and the lamellae, MC sizes generated by histology were close but *larger* than those measured by mucosal mapping. This again was because of non-random selection of the very few MCs on these generally healthy gill respiratory surfaces and the non-random cell profiles in transverse sections vs unbiased selection from tangential sections, representing a larger organ surface. While both the unbiased size of the skin MCs (M7) and the unbiased lamellar MC density (M5) could distinguish between stations (pollution levels), only the histological measure of number of cells per interlamellar unit (H1) could do the same (Table 1).

The differences in MC density between traditional MC count and mucosal mapping in this study is the distinction between numerical and volumetric density of MCs in the mucosal epithelium. While in traditional transverse sections, a numerical density of MCs can be counted from the visible cells along a linear transect, the mucosa *thickness* can be vastly different between species and between organs, thus affecting counts and numerical density. This effect can be minimized if many transverse sections are observed, however, it will be time consuming. Furthermore, 10 sections of 100 μm thickness give us 1 mm of surface area, serial or not, and still does not represent a great deal of the surface area. A numerical density means how many cells in this volume of tissue: here we have two “red herring” in that i) 5 small cells are numerically higher than 1 large cell but may be physiological less important than that large one, and ii) the variable thickness of the mucosal epithelium on species and organs can be affected by handling, sampling, transport, rearing system, species and just plain touching by accident, so this is not a static measure, ever, and reflects instead the necessarily regenerative state of this protective barrier. A volumetric density states clearly how much mucous cells in a given amount of epithelium, regardless of its “thickness”. Volumetric density shows the interaction between the size and number of the mucous cells in the reference volume of the mucosa and is thus directly comparable across tissues.

4.1. Orientation and number of analysed mucous cells

Regarding quantification of the gill MCs, the main difference is that traditional methods only quantify MCs on well-oriented filaments whereas mucosal mapping could employ any orientation. Subsequently, the total number of MCs quantified by mucosal mapping (1948 MCs on filament and 172 MCs on lamellae) was more than 5 times greater than those measured by traditional method (336 MCs on filament and 59 MCs on lamellae). However, the distinction between filament and lamellar MC sizes was obtained even with much fewer measures from each of many more gill sections [47,48]. The use of optimal orientation of the sections to be measured usually require the fish be killed for sampling, whereas mucosal mapping is independent of section orientation and opens for *in vivo* estimates of MC responses (for example biopsy samples) for assessment of fish health. We conducted an ethical trial of *in vivo* biopsies of skin and gills on 80 salmon smolt, where 30 were subjected to gill clips (small pieces of the second gill cut by surgical scissors falling into the histocassette below). Despite the completely random orientation of the filaments and lamellae, the resultant measures gave good reproducibility for both filament and lamella, and all the fish survived and showed signs of regenerating the gill tissue. The skin biopsies of about 8 mm diameter gave good reproducibility for the measures, but application of 4 types of wound healing substances was counterproductive – all the treated wounds expanded over time whereas those without any wound covering remained near the biopsy size while regenerating. Unfortunately, there was also some inflammation in the underlying muscle tissue and so this *in vivo* skin biopsy prospect was abandoned. However, gill clips work fine for measuring gill mucosa and separates reliably measures on lamellae and filament (Pittman, Brennan, Powell, Andersen and Blindheim, unpub results, presented at the Gill Health Initiative in Bergen, 2018). The second gill arch was chosen for convention and fit with general fish health practices.

For skin samples, due to tangential orientation of sectioning, mucosal mapping was able to examine a larger area of epithelium compared to traditional method where transversal sections were used for quantification. As a result, total number of MCs measured by the mucosal mapping (5788 MCs) was nearly 5 times greater than number of MCs measured by the traditional method (1224 MCs, Table 1). Variation of measurements within the same fish varied among mucosal indices. For examples, mucosal mapping indices (M1-M9) or number of MCs per ILU (H1) did not vary much whereas size of skin MCs (H7) varied a lot even within the same photos. As the effect sizes of related tests were considered to be large, the use of 25 counter frames (instead of 50 counter frames) was enough to generate representative mucosal mapping indices (M1-M9) per fish. Significant differences between treatments can be obtained with unbiased selection of as few as 50–100 cells per section in mucosal mapping [26,33]. Variation in number of MCs per ILU (H1) was smallest in all traditional mucosal indices. The use of 10 photos per fish was adequate to result powers of over 0.8.

4.2. Pollutant exposure

Mucosal barriers are important when assessing effects from environmental stressors on fish [8] and traditional MCs counts are commonly used to investigate MC responses to environmental challenges [49–51]. For example, in shorthorn sculpin from East Greenland, number of MCs/ILU in fish from the Pb–Zn polluted site (0.27 ± 0.55) was significantly greater than that in fish from reference site (0.13 ± 0.39) [32]. In rainbow trout (*Oncorhynchus mykiss*) fry 2 months post hatching, limited exposure to formalin (50 ppm for 1 h) resulted in an increase in numerical density of MCs whereas an extended exposure to formalin (200–300 ppm for 1 h or 50 ppm for 24 h) decreased MC density [30]. Numerical density of MCs in gills (cell/mm^2 of gill section area) of tilapia (*Oreochromis* sp.) exposure to Cd (4.45 μM) at various time point (0 h–15 days) increased significantly after 5 h of exposure but not after 5 and 15 days [31]. In this study, both traditional count and mucosal map detected statistically significant differences among stations with different levels of Pb contamination.

Regarding mucosal indices generated using traditional MC counts, only number of MCs/ILU of gills (H1) differentiated shorthorn sculpin from various stations with different levels of pollution. As ILU is not constant across species nor within a species at different oxygen, ammonia, salinity or temperature levels [52], the number of MC/ILU (H1) for health assessment of fishes needs to be interpreted with caution. There was no association between any traditional mucosal indices (H1 – H7) and concentrations of Pb in liver.

Mucosal mapping revealed the significant difference in shorthorn sculpins from stations with various level of Pb and Zn in volumetric density of lamellar MCs (M5) and size of skin MCs (M7) [29]. Significant positive correlation was found between level of hepatic Pb and size of MCs on filament (M1) and lamellae (M4) [29]. This indicates that mucosal mapping indices have biomarker potentials for chronic exposure to Pb. The variation in sensitivity between traditional MC count and mucosal mapping may relate to the selection method for the number of MCs included in each measurement.

4.3. Parasitic infections

The interactions between fish mucosa with ectoparasites and some endoparasites such as gastrointestinal helminths are dynamic [53–55]. Fish commonly respond to ectoparasitic infection by increasing mucus secretion [56]. If parasitic infections overwhelm host responses, the number of MCs would decrease, indicating an exhausted status [21,53,54,57]. For example, traditional MCs count detected a decrease in a number of skin MCs of brown trout (*Salmo trutta fabrio*) or rainbow trout (*Oncorhynchus mykiss*) infected at high levels of ectoparasites (*Gyrodactylus colemanensis:* 95–100/fish, *G. derjavini;* 0.48–13.67/cm^2 and *Lepeophtheirus salmonis:* 3–10/fish) [21,53,54,57]. If parasitic infection did not overwhelm fish's resources, the fish would respond to retain the balance between host and pathogens. Mucosal mapping results pointed out that shorthorn sculpins were able to maintain stable skin MC volumetric densities (M8) between three stations and skin barrier status of these fish positively correlated with number of trematodes, a skin parasite (M9) [29]. In this study, traditional counts of skin MCs of shorthorn sculpin did not show any links with the levels of parasitic infection perhaps because the parasitic infection did not overwhelm host's responses.

The size of gill filament MCs (H3) measured in the present study by the traditional method was negatively associated with parasitic infections while gill mucosal indices generated by mucosal mapping did not correlate with parasitic infections. It is important to note that in this paper the parasite load data were standardized from the number of parasites observed from the histological sections (sampled gill arch or skin) [29]. A large number of Trichodinid (up to 33 parasites per filament) was commonly found within inter-lamellar units of the gills of the fish from all stations [29]. Metacercarie, a stage of digenea parasite, located within histological sections of skin (in the dermis and underlying muscle) [29]. The variation due to the distance between histological samples and the parasites was not significant in this study as only parasite that was next to or in histological sections was included in statistical analyses. As traditional methods only investigated the MC on the edge of filament when surrounded by lamellae which may be a haphazard result of plane of sectioning, while mucosal mapping included any filament area regardless of the presence of lamellae. There are thus two interpretations:

- that ILU (which is very different from species to species) comprises representatives of *both* filamentous and lamellar cell populations, somewhat haphazardly mixed according to plane of sectioning. This is supported by the comparison of cell sizes generated by each method and testing for significant differences.
- that the increased presence of well-oriented lamellae surrounding a MC on the filament is an artefact of generally increased filament MC density and will appear irregularly to bias results.

4.4. Organ specificity of MC indices

Both methods distinguished significantly larger and denser (numeric vs volumetric) skin MCs compared to those on gills. Variations between different MC populations from various organs were also reported in other fish species. For example, in European seabass (*Dicentrarchus labrax)*, MCs in the skin (dorsal area) were significantly larger in size but lower in density compared to those in gut [26]. In Atlantic salmon (*Salmo salar*), skin MCs on head, dorsolateral and caudal peduncle sites of skin were significantly different in both size and volumetric density [25]. Volumetric density of MCs in the skin was lowest at caudal and highest at the dorsal area in Atlantic salmon [25]. Similarly, in rainbow trout, MC numeric density varied significantly among body sites. The lowest MC numeric density was found on caudal fin and corneal surface whereas the highest density was on the body, pectoral fin and dorsal fin [53]. Measures of MC density from standard histology usually mean “numeric density” or the number per selected unit [27,49,53,58]. Not only does this obfuscate the importance of actual size (are 5 cells of 24 μ^2 more or less than 1 cell of 120 μ^2), numeric density is insensitive to any size changes which may accompany acute or enhanced responses [26], as well as the changes in volumetric density which would accompany exhaustion or chronic activation of the mucosal barrier (eg from gastrointestinal parasites). Thus, numerical density has limited application to the understanding of mucosal dynamics when it is in the absence of a valid reference volume.

While the traditional method did not reveal any differences between filament and lamellar MCs, mucosal mapping did. The dissimilarity of

MC populations from filament and lamellae was also reported in Atlantic salmon at both prior and after hydrogen peroxide or peracetic acid exposure using mucosal mapping method [47,48]. Differences in size and density of MCs from various locations suggested that they may have separate functions or origins. Sizes of MCs in gill lamellae of Atlantic salmon exposed to 0.06 and 1.2 ppm peracetic acid (PAA) were significant greater than those cells on fish treated with 2.2 ppm PPA whereas MCs on the gill filaments of those fish were not significantly altered among treatments [48]. The positive correlation between hepatic Pb and size of filament MCs, but not skin or lamellar MCs, suggested that filament MCs may play a role in reducing the load of Pb in shorthorn sculpin [29]. Rainbow trout (*Oncorhynchus mykiss*) experimentally infected with *Ichthyophthirius multifilii*, mucosal immunoglobin response (tpIgR) showed markedly expressed in filaments and only a few were in lamellae [59]. This suggested that MCs on filaments and lamellae of rainbow trout play alternative functions, with lamellae representing the respiratory surface and, perhaps, the filament representing more systemic health.

4.5. Body size

Traditional MC measures of shorthorn sculpins were closely associated with their body size (Table 2). More specifically five out of seven mucosal indices generated by traditional method (H1, H2, H4, H5 and H7) moderately to strongly correlation with either or all body size categories including length, weight and liver weight. About 50% (11/21) of investigated correlations were statistically significant. Similarly, four out of nine mucosal indices measured by mucosal mapping (M2, M3, M7 and M8) were associated with body size resulting in about one-third of investigated relationships being statistically significant. Both traditional measurement and mucosal mapping agreed that shorthorn sculpins mucous cell responses were closely associated with body size of the fish. Off all investigated mucosal indices, number of MC/cm filament (H1), size of skin MCs (H7), filament MC density (M2) and filament barriers (M3) were the safest mucosal indicators for the fish body size. Additionally, the two methods agreed that gill mucosal indices positively correlated with body size whereas skin mucosal indices were negatively associated with body size. Also, mucosal mapping indicated that MCs in the filament were related to body size whereas those in the lamellae were not. These variations supported the hypothesis that different MC populations may have distinct origins or play alternative functions [25,26,29,47,48].

4.6. Detection of parasites

The sampling and processing protocols used in mucosal mapping were efficient to investigate infection levels with skin parasites as the larger surface areas were examined. Additionally, as the collected samples were put into pre-labelled histocassettes before fixation, the detachment of parasites during fixation, transportation and processing was reduced. The fact is that although only a small area of skin (about 1 cm^2) was examined, this method detected a digenean infection in 43% of sampled fish with maximum intensity reaching 10 digenea/cm^2 [29]. Future studies that investigate interactions between quantitative mucosal responses and parasitic loads on skin may focus on more standardized sites of skin samples (larger samples at multiple sites) per fish.

Traditional counts provided a good overview of skin layers, allowed to locate parasites in whether epithelium, dermis or muscle. These characteristics provide important information for identification of the parasites especially when histological samples were the only available materials.

4.7. Health implication

Both traditional quantification of MCs and mucosal mapping agreed that the mucosal barriers in the gills and skin of shorthorn sculpin from Maarmorilik, West Greenland were affected by environmental challenges including pollutant exposure and parasitic infection. This suggested that immune functions, an important indication of general health in fish, of shorthorn sculpins in this area were not exhausted [29]; this study). Some variations of MC responses depicted by each method were listed below:

- Traditional methods differentiated two MC populations: one in the skin and the other in the gills. MC population in the gills (H1 and H3) was responsive to pollutants and trichodinid, a gill parasite. MCs in the skin did not respond to either pollutants or parasites. Both MC populations change with size of the fish.
- Mucosal mapping separated three MC populations in the gill filaments, gill lamellae and skin. Both MC populations in the gill (M1, M4, M5) were related to pollution where MCs in the skin (M9) changed with the number of trematodes, a skin parasite [29]. MCs of all population linked with fish size.

Finally, it is important to note that the samples were from a field study where a number of other factors such as diet, water quality or other pathogens can contribute to MC responses. Laboratory controlled experiments where all potential factors can be controlled are recommended to confirm the potential causations between MCs, pollutants and parasites. Here, we focus on the differences between the two methods used to measure MC responses from the same set of samples. The results will be highly valuable in future assessment of mucosal barriers, important components of fish health.

5. Conclusion

Overall, the histological measurement and mucosal mapping showed different MC patterns among sculpin from Pb contaminated stations and detected links between MC responses and parasitic infections. Traditional quantification was mostly related to the body size of fishes whereas mucosal mapping detected the link between MC responses and Pb level in liver. The two methods were able to distinguish MC population in skin from those in the gills, but only mucosal mapping pointed out the differences between filament and lamellar MC populations within the gills. The use of optimal orientation of the gill sections to be measured in traditional methods would usually require the fish be killed for sampling, whereas mucosal mapping is independent of section orientation and opens for *in vivo* estimates of MC responses (for example biopsy samples) for assessment of fish health. Of all traditional mucosal indices (from H1 to H7), number of MCs per ILU (H1) was the most reliable whereas number of MC per cm length of skin (H6) was less reliable than the other indices. The use of all three mucosal mapping indices (size, density and barrier status) is recommended for an insight on status and dynamic of each MC population. The use of both traditional and mucosal mapping methods in field studies would promise of a holistic understanding on MCs responses and their associations with body size, hepatic Pb and parasitic infection especially with different MC populations, while mucosal mapping lends itself to inclusion in studies of environmental impacts on fish immunology.

CRediT authorship contribution statement

Mai Dang: Conceptualization, Methodology, Validation, Formal analysis, Investigation, Writing - original draft. **Karin Pittman:** Conceptualization, Methodology, Validation, Formal analysis, Investigation, Resources, Writing - review & editing, Supervision, Funding acquisition. **Christian Sonne:** Investigation, Resources, Writing - review & editing, Funding acquisition. **Sophia Hansson:** Investigation, Resources, Writing - review & editing. **Lis Bach:** Investigation, Resources, Writing - review & editing, Funding acquisition. **Jens Søndergaard:** Investigation, Resources, Writing - review &

editing, Funding acquisition. **Megan Stride:** Investigation, Resources, Writing - review & editing, Supervision. **Barbara Nowak:** Conceptualization, Investigation, Resources, Writing - review & editing, Supervision, Project administration, Funding acquisition.

Declaration of competing interest

Author Pittman developed mucosal mapping in 2010 [24] which has since been made commercially available as Veribarr TM, under Quantidoc AS where she is Chief Scientific Officer.

Acknowledgments

The University of Tasmania is acknowledged for funding Mai Dang's PhD. The Australian Society for Parasitology is acknowledged for supporting the first author's trip to Norway to analyse samples (JD Smyth Postgraduate Student Travel Award 2017).

The authors would like to acknowledge The Ministry of Environment and Food of Denmark, Aarhus University, The Environmental Agency for Mineral Resource Activities (project 771020), Government of Greenland, the Arctic Research Centre and the mining company Angel mining PLC for supporting the field trip by which our archival samples were collected. The authors sincerely thank Dr. Grigory Merkin and Dr. Mearge Okubamichael (Quantidoc AS, Bergen, Norway) for their guidance and assistance during the analyses using mucosal mapping techniques. Dr. Mach Diep, Dr. Nguyen Thi Hai Thanh, Dr. Le Hoang Thi My Dung, and Dr. Mei Ooi are acknowledged for their support during the Norway trip and the development of this manuscript.

References

[1] M. Maita, Fish health assessment, in: H. Nakagawa, M. Sato, I.I.I.D.M. Gatlin (Eds.), Dietary Supplements for the Health and Quality of Cultured Fish, CAB International, 2007, pp. 10–34.
[2] V.S. Blazer, H.L. Walsh, R.P. Braham, C. Smith, Necropsy-based wild fish health assessment, JoVE 2018 (2018) 1–11, https://doi.org/10.3791/57946.
[3] M. Braceland, K. Houston, A. Ashby, C. Matthews, H. Haining, H. Rodger, P.D. Eckersall, Technical pre-analytical effects on the clinical biochemistry of Atlantic salmon (*Salmo salar* L.), J. Fish. Dis. 40 (2017) 29–40, https://doi.org/10.1111/jfd.12476.
[4] R.J. Roberts, Fish Pathology, John Wiley & Sons, 2012.
[5] C.J. Secombes, A.E. Ellis, The immunology of teleost, in: R. Roberts (Ed.), Fish Pathology, Wiley-Blackwell, 2012, pp. 144–166.
[6] C.C. Lazado, C.M.A. Caipang, Mucosal immunity and probiotics in fish, Fish Shellfish Immunol. 39 (2014) 78–89, https://doi.org/10.1016/j.fsi.2014.04.015.
[7] S. Dash, S.K. Das, J. Samal, H.N. Thatoi, Epidermal mucus, a major determinant in fish health: a review, Iran. J. Vet. Res. 19 (2018) 72–81.
[8] N.A.R. Cabillon, C.C. Lazado, Mucosal barrier functions of fish under changing environmental conditions, Fishes (2019) 1–10, https://doi.org/10.3390/fishes4010002.
[9] J.B. Claiborne, S.L. Edwards, A.I. Morrison-Shetlar, Acid-base regulation in fishes: cellular and molecular mechanisms, J. Exp. Zool. 293 (2002) 302–319.
[10] D.H. Evans, Cell signaling and ion transport across the fish gill epithelium, J. Exp. Zool. 293 (2002) 336–347.
[11] D.H. Evans, P.M. Piermarini, K.P. Choe, The multifunctional fish gill: dominant site of gas exchange, osmoregulation, acid-base regulation, and excretion of nitrogenous waste, Physiol. Rev. 85 (2005) 97–177.
[12] H.W. Ferguson, Systemic Pathology of Fish. A Text and Atlas of Comparative Tissue Responses in Diseases of Teleosts, Scotian Press, London, 2006.
[13] F. Genten, E. Terwinghe, A. Danguy, Atlas of Fish Histology, Science Publishers, Enfield, NH, 2009.
[14] J. Mallatt, Fish gill structural changes induced by toxicants and other irritants: a statistical review, Can. J. Fish. Aquat. Sci. 42 (1985) 630–648.
[15] D.E. Hinton, P.C. Baumann, G.R. Gardner, W.E. Hawkins, J.D. Hendricks, R.A. Murchelano, M.S. Okihino, Histopathologic biomarkers, in: R.J. Huggett, R.A.P.M.M. Kimerle, Jr.H.L. Bergman (Eds.), Biomarker Biochemical, Physiological and Histological Marker of Anthropogenic Stress, Lewis publishers, Boca Raton, 1992, pp. 155–209.
[16] A.M. Abdel-Moneim, M.A. Al-Kahtani, O.M. Elmenshawy, Histopathological biomarkers in gills and liver of *Oreochromis niloticus* from polluted wetland environments, Saudi Arabia, Chemosphere 88 (2012) 1028–1035.
[17] I.D. Gomes, A.A. Nascimento, A. Sales, F.G. Araújo, Can fish gill anomalies be used to assess water quality in freshwater Neotropical systems? Environ. Monit. Assess. 184 (2012) 5523–5531.
[18] A.A. Nascimento, F.G. Araújo, I.D. Gomes, R.M.M. Mendes, A. Sales, Fish gills alterations as potential biomarkers of environmental quality in a eutrophized tropical river in South-Eastern Brazil, Anat. Histol. Embryol. 41 (2012) 209–216.
[19] J.M. McKim, G.J. Lien, Toxic responses of the skin, in: D. Schlenk, W.H. Benson (Eds.), Target Organ Toxicity in Marine and Freshwater Teleosts, vol. 1, Taylor & Francis, 2001, pp. 151–223 *Organs*.
[20] R.H. Easy, N.W. Ross, Changes in Atlantic salmon (*Salmo salar*) epidermal mucus protein composition profiles following infection with sea lice (*Lepeophtheirus salmonis*), Comp. Biochem. Physiol. Genom. Proteonomics 4 (2009) 159–167, https://doi.org/10.1016/j.cbd.2009.02.001.
[21] K.L. Shephard, Functions for fish mucus, Rev. Fish Biol. Fish. 4 (1994) 401–429, https://doi.org/10.1007/BF00042888.
[22] P. Alvarez-Pellitero, Fish immunity and parasite infections: from innate immunity to immunoprophylactic prospects, Vet. Immunol. Immunopathol. 126 (2008) 171–198, https://doi.org/10.1016/j.vetimm.2008.07.013.
[23] S. Rakers, L. Niklasson, D. Steinhagen, C. Kruse, K. Sundell, R. Paus, Antimicrobial peptides (AMPs) from fish epidermis : perspectives for investigative dermatology, J. Invest. Dermatol. 133 (2013) 1140–1149, https://doi.org/10.1038/jid.2012.503.
[24] K. Pittman, P. Sourd, B. Ravnøy, Ø. Espeland, I.U. Fiksdal, T. Oen, A. Pittman, K. Redmond, J. Sweetman, Novel method for quantifying salmonid mucous cells, J. Fish. Dis. 34 (2011) 931–936, https://doi.org/10.1111/j.1365-2761.2011.01308.x.
[25] K. Pittman, A. Pittman, S. Karlson, T. Cieplinska, P. Sourd, K. Redmond, B. Ravnøy, E. Sweetman, Body site matters: an evaluation and application of a novel histological methodology on the quantification of mucous cells in the skin of Atlantic salmon, *Salmo salar* L, J. Fish. Dis. 36 (2013) 115–127, https://doi.org/10.1111/jfd.12002.
[26] S. Torrecillas, D. Montero, M.J. Caballero, K.A. Pittman, M. Custódio, A. Campo, J. Sweetman, M. Izquierdo, Dietary mannan oligosaccharides: counteracting the side effects of soybean meal oil inclusion on European seabass (*Dicentrarchus labrax*) gut health and skin mucosa mucus production? Front. Immunol. 6 (2015) 397, https://doi.org/10.3389/fimmu.2015.00397.
[27] M.D. Fast, D.E. Sims, J.F. Burka, A. Mustafa, N.W. Ross, Skin morphology and humoral non-specific defence parameters of mucus and plasma in rainbow trout, coho and Atlantic salmon, Comp. Biochem. Physiol. Mol. Integr. Physiol. 132 (2002) 645–657, https://doi.org/10.1016/S1095-6433(02)00109-5.
[28] M. Dang, R. Nørregaard, L. Bach, C. Sonne, J. Søndergaard, K. Gustavson, P. Aastrup, B. Nowak, Metal residues , histopathology and presence of parasites in the liver and gills of fourhorn sculpin (*Myoxocephalus quadricornis*) and shorthorn sculpin (*Myoxocephalus scorpius*) near a former lead-zinc mine in East Greenland, Environ. Res. 153 (2017) 171–180.
[29] M. Dang, K. Pittman, L. Bach, C. Sonne, S.V. Hansson, J. Søndergaard, M. Stride, B. Nowak, Mucous cell responses to contaminants and parasites in shorthorn sculpins (*Myoxocephalus scorpius*) from a former lead-zinc mine in West Greenland, Sci. Total Environ. (2019) 207–216.
[30] K. Buchmann, J. Bresciani, C. Jappe, Effects of formalin treatment on epithelial structure and mucous cell densities in rainbow trout, *Oncorhynchus mykiss* (Walbaum), skin, J. Fish. Dis. 27 (2004) 99–104, https://doi.org/10.1111/J.1365-2761.2003.00519.X.
[31] S.M. Wu, M.J. Shih, Y.C. Ho, Toxicological stress response and cadmium distribution in hybrid tilapia (*Oreochromis* sp.) upon cadmium exposure, Comp. Biochem. Physiol. C Toxicol. Pharmacol. 145 (2007) 218–226, https://doi.org/10.1016/j.cbpc.2006.12.003.
[32] R.D. Nørregaard, M. Dang, L. Bach, O. Geertz-Hansen, K. Gustavson, P. Aastrup, P.S. Leifsson, J. Søndergaard, B. Nowak, C. Sonne, Comparison of heavy metals, parasites and histopathology in sculpins (*Myoxocephalus* spp.) from two sites at a lead-zinc mine in North East Greenland, Environ. Res. 165 (2018) 306–316, https://doi.org/10.1016/j.envres.2018.04.016.
[33] K. Pittman, A. Campo, S. Karlson, A. Pittman, J. Johansen, P. Sourd, Ø. Espeland, E. Sweetman, B. Ravnøy, Mucosal Mapping and its Importance in Fish Farming, European Aquaculture Society, Trondheim, Norway, 2013.
[34] K. Pittman, M. Okubamichael, G. Merkin, S. Haddeland, C.C. Lazado, T. Jonassen, S. Øyen, K. Korsnes, M. Powell, N. Sissener, L. Andersen, A. Bogevik, M. Dang, B. Nowak, K. Kousoulakis, A. Lyngøy, M. Oj, Quantified mucosal health of fishes : the proposed " rules .", 1st International Symposium On Mucosal Health In Aquaculture (MHA2019), 2019, pp. 2–4 (Oslo, Norway).
[35] M. Kipp, M.C. Kiessling, T. Hochstrasser, C. Roggenkamp, C. Schmitz, Design-based stereology for evaluation of histological parameters, J. Mol. Neurosci. 61 (2017) 325–342, https://doi.org/10.1007/s12031-016-0858-9.
[36] SV Hansson, J Søndergaard, L Bach, V Hansen, C Sonne, CJ Jørgensen, J Nymand, A Mosbech, Environmental monitoring at mine sites in Greenland. A review of research and monitoring practices and their role in minimizing environmental impact, Aarhus University, DCE – Danish Centre for Environment and Energy, Aarhus, Denmark, 2020 44 Pp. Scientific Report No. 364, Aarhus University.
[37] S.V. Hansson, J.-P. Desforges, F.M. van Beest, L. Bach, N. Halden, C. Sonne, A. Mosbech, J. Søndergaard, Bioaccumulation of mining derived metals in blood, liver, muscle and otoliths of two Arctic predatory fish species (*Gadus ogac and Myoxocephalus scorpius*), Environ. Res. (2020) 109194, https://doi.org/10.1016/j.envres.2020.109194.
[38] E.L. Lewis, R.G. Perkin, Seasonal mixing processes in an arctic fjord system, J. Phys. Oceanogr. 12 (1982) 74–83, https://doi.org/10.1175/1520-0485(1982)012<0074:smpiaa>2.0.co;2.
[39] B. Thomassen, The Black Angel lead-zinc mine at Maarmorilik in west Greenland, Geol. ore 2003 (2003) 12.
[40] B. Elberling, G. Asmund, H. Kunzendorf, E.J. Krogstad, Geochemical trends in metal-contaminated fiord sediments near a former lead-zinc mine in West Greenland, Appl. Geochem. 17 (2002) 493–502, https://doi.org/10.1016/S0883-

2927(01)00119-6.
[41] K. Perner, T. Leipe, O. Dellwig, A. Kuijpers, N. Mikkelsen, T.J. Andersen, J. Harff, Contamination of Arctic fjord sediments by Pb-Zn mining at Maarmorilik in central West Greenland, Mar. Pollut. Bull. 60 (2010) 1065–1073, https://doi.org/10.1016/j.marpolbul.2010.01.019.
[42] S.D. Roberts, M.D. Powell, Comparative ionic flux and gill mucous cell histochemistry: effects of salinity and disease status in Atlantic salmon (*Salmo salar* L.), Comp. Biochem. Physiol. Mol. Integr. Physiol. 134 (2003) 525–537.
[43] B. Nowak, K. Cadoret, S.W. Feist, T.P. Bean, Laser-capture dissection and immunohistochemistry reveals chloride and mucous-cell specific gene expression in gills of seawater acclimated Atlantic salmon Salmo salar, J. Fish. Biol. 83 (2013) 1459–1467.
[44] M.D. Powell, D.J. Speare, G.M. Wright, Morphological changes in rainbow trout (*Oncorhynchus mykiss*) gill epithelia following repeated intermittent exposure to chloramine-T, Can. J. Zool. 73 (1995) 154–165.
[45] D.A. Peterson, Quantitative histology using confocal microscopy: implementation of unbiased stereology procedures, Methods: A Companion to Methods in Enzymol 18 (1999) 493–507, https://doi.org/10.1006/meth.1999.0818.
[46] V. Howard, M. Reed, Unbiased Stereology: Three-Dimensional Measurement in Microscopy, Garland Science/BIOS Scientific Publishers, 2004.
[47] I. Rantty, K. Pittman, E. Sweetman, Delousing with Hydrogen Peroxide: Skin, Gills and Esophagous Responses and Repair in the First Three Weeks after Treatment. Masters Degree in Aquaculture Biology, University of Bergen, 2016.
[48] S. Haddeland, Benchmarking Healthy Gills in Atlantic Salmon (*Salmo salar*) in Seawater Recirculating Aquaculture System after Repeated Peracetic Acid Exposure, (2019).
[49] K. Ledy, L. Giambérini, J.C. Pihan, Mucous cell responses in gill and skin of brown trout *Salmo trutta* fario in acidic, aluminium- containing stream water, Dis. Aquat. Org. 56 (2003) 235–240.
[50] I.N. Vatsos, Y. Kotzamanis, M. Henry, P. Angelidis, M.N. Alexis, Monitoring stress in fish by applying image analysis to their skin mucous cells, Eur. J. Histochem. 54 (2010) 107–111, https://doi.org/10.4081/ejh.2010.e22.
[51] L.B. Jensen, S. Boltana, A. Obach, C. McGurk, R. Waagbø, S. MacKenzie, Investigating the underlying mechanisms of temperature-related skin diseases in Atlantic salmon, *Salmo salar* L., as measured by quantitative histology, skin transcriptomics and composition, J. Fish. Dis. 38 (2015) 977–992, https://doi.org/10.1111/jfd.12314.
[52] K.M. Gilmour, S.F. Perry, Conflict and compromise: using reversible remodeling to manage competing physiological demands at the fish gill, Physiology 33 (2018) 412–422, https://doi.org/10.1152/physiol.00031.2018.
[53] K. Buchmann, J. Bresciani, Microenvironment of *Gyrodactylus derjavini* on rainbow trout *Oncorhynchus mykiss*: association between mucous cell density in skin and site selection, Parasitol. Res. 84 (1998) 17–24, https://doi.org/10.1007/s004360050350.
[54] D.T. Nolan, P. Reilly, S.E.W. Bonga, Infection with Low Numbers of the Sea Louse *Lepeophtheirus salmonis* Induces Stress-Related Effects in Postsmolt Atlantic Salmon (*Salmo salar*) vol. 959, (1999), pp. 947–959.
[55] C. Sharpe, D.J. Thornton, R.K. Grencis, A sticky end for gastrointestinal helminths ; the role of the mucus barrier, Parasite Immunol. (2018) 1–10, https://doi.org/10.1111/pim.12517.
[56] J. Lom, I. Dyková, Protozoan Parasites of Fishes, Elsevier Science Publishers, Amsterdam, 1992 Elsevier.
[57] P.R. Wells, D.K. Cone, Experimental Studies on the Effect of of *Gyrodactylus colemanensis* and *G. Salmonis* (Monogenea) on Density of Mucous Cells in the Epidermis of Fry of *Oncorhynchus mykiss*, (1990), pp. 599–603.
[58] A. Pickering, The distribution of mucous cells in the epidermis of the brown trout *Salmo trutta* (L.) and the char *Salvelinus alpinus* (L.), J. Fish. Biol. 6 (1974) 111–118, https://doi.org/10.1111/j.1095-8649.1974.tb04531.x.
[59] Z. Xu, F. Takizawa, D. Parra, D. Gómez, L. Von Gersdorff Jørgensen, S.E. Lapatra, J.O. Sunyer, Mucosal immunoglobulins at respiratory surfaces mark an ancient association that predates the emergence of tetrapods, Nat. Commun. 7 (2016), https://doi.org/10.1038/ncomms10728.